

Tilted Leg Design for a Rapid-Prototyped Low-Voltage Piezoelectric Running Robot

Ketul Patel
Dept. of Mechanical Engineering
University of Michigan
Ann Arbor, MI, USA
ketul@umich.edu

Jinhong Qu
Dept. of Mechanical Engineering
University of Michigan
Ann Arbor, MI, USA
jinhongq@umich.edu

Kenn R. Oldham
Dept. of Mechanical Engineering
University of Michigan
Ann Arbor, MI, USA
oldham@umich.edu

Abstract—This paper describes design and experimental testing of a simple rapid-prototyped, piezoelectrically-actuated legged robot. The 2 cm long by 3 cm wide robot is intended to serve as a large-scale testbed for concepts applicable to millimeter-scale, thin-film piezoelectrically-actuated micro-robots. It achieves high-speed, low-voltage operation through tilted orientation of cantilever-like legs. Tethered locomotion is achieved at 36 mm/s (> 1 body length per second) at as little as 10 V or at speeds as large 400 mm/s at 80 V. Electronic loading characteristics of the piezoelectric actuators at low voltage conditions are similar to those of millimeter-scale prototypes. Free dynamics of the robot feet are measured experimentally to gain further insight into cantilever orientation effects on locomotion speed.

Keywords- Piezoelectric Actuation, Rapid Prototyping, Legged Locomotion

I. INTRODUCTION

In recent years, many miniature terrestrial walking or running robots have been demonstrated at scales of approximately 10 cm or smaller. Such robots have been produced by a variety of manufacturing techniques, ranging from low-cost 3D printing [1] [2] [3] to novel soft printing [4] [5] [6], folded laminate construction [7] [8] [9], and other fabrication techniques [10] [11] [12]. Perhaps the highest performance robots at this scale, in terms of locomotion speed, have relied on small, conventional electromagnetic motors [13] [9] [14]. However, piezoelectric materials hold significant interest for small robots due to both their large energy density and reasonable efficiency, having been used in several of the other robots above. In addition, piezoelectric materials may provide benefits for further downward scaling of miniature terrestrial robots [15] [16] [17].

Piezoelectrically-actuated robots at this scale have typically faced a few major limitations. First, piezoelectric materials are generally readily available only as planar beams or sheets, with most easily-excited motions perpendicular to the material plane. To generate a combination of vertical and lateral motion in legged robots from such materials, several strategies have been

proposed. These include use of folded mechanisms constructed from other materials [8], laser cutting of geometries permitting differential actuation on opposite sides of a robot foot [11], placement of structures at critical locations relative to modal nodes and anti-nodes [10], and assembly of piezoelectric elements to asymmetric leg architectures [1]. Second, voltage requirements for piezoelectric materials are typically large, ranging from 25 V to over 100 V among the robots described above. This leads to increased complexity in robot integration with power sources and power electronics that may be difficult to scale in size, especially when a robot is intended to operate on battery power.

This paper presents an empirical evaluation of certain simple strategies to reduce centimeter-scale piezoelectric running robot voltage requirements and/or increase robot speed through departure from purely planar piezoelectric arrangements. In this work, robots were to be assembled from off-the-shelf piezoelectric components and 3D-printed parts, for rapid prototyping and experimentation. The authors have previously used similar assembly techniques to study dynamic contact models for small-scale robots [1] [2] [18]. This has helped to better understand the effects of complex interactions of robot vibratory dynamics and impact events in determining small robot locomotion effectiveness. In this work, installation of piezoelectric element on tilted/angled beam structures to produce robot legs is shown to successfully produce locomotion at voltages as low as 10 V. Resulting robots have power and energy requirements much more comparable to millimeter-scale, microelectromechanical system (MEMS)-based piezoelectric robots, and may be useful as testbeds for power management and control systems. In addition, analysis of robot foot profiles provides some qualitative insight into coupling of lateral and vertical foot motions that are advantageous at the centimeter scale.

II. LEG DESIGN AND FABRICATION

Rapid-prototyped robot designs were evaluated with the goal of providing high-speed, low-voltage operation using off-the-shelf piezoelectric materials and generally available 3D printing technology. Piezoelectric elements were selected as

The authors thank the National Science Foundation, award CMMI 1435222, for support of this work.
XXX-X-XXXX-XXXX-X/XX/\$XX.00 ©20XX IEEE

brass-reinforced lead-zirconate-titanate (PZT) bimorphs (Piezo Systems, T219-A4CL-103X). Such bimorphs were selected due to their combination of small size (3 mm x 28 mm) and modest expense. Initial prototyping was performed with 3D-printed polylactic acid (Ultimaker), with later iterations using Visijet M3 Crystal resin (3D Systems).

A. Concept Generation

Prior microrobot prototypes generated by the authors and their collaborators using the components above have been designed with six legs connected to a comparatively rigid body [1]. They featured a cantilever beam leg geometry actuated using bimorph piezoelectric ceramic strips. These strips were attached to each beam with a vertical, rigid foot at the tip. Vertical motion of the legs lifts the robot body against gravity, while the in-plane motion make the bot move the robot forward. In-plane actuation was achieved either by placing the piezoelectric strip asymmetrically on the cantilever beam, or by attaching a cantilever on both sides of each foot to produce a torsional rotation of the foot, also reminiscent of the strategy in [11]. Each leg used a single piezoelectric ceramic.

In this work, robot forward motion is sought by attaching the bimorph piezoelectric ceramic strips at an angle or tilt relative to the body. This distributes forces/moments from the piezoelectric material in both the vertical and lateral directions as defined by the robot chassis or body. The force distribution is determined to the angle they are attached.

Three different designs were developed for full experimental testing. They are compared to a robot of very similar geometry but fully-planar legs, assembled as in past work. Figure 1 shows an illustrative photograph of an assembled robot, while Fig. 2 shows the rendered images of all three tilted-leg prototype bots. The first design (Fig. 2(a)) has six legs and a slope of 10° on the legs. This slope was created to place the bimorph piezoelectric ceramic strip at an angle. To study how the angle of inclination changes the performance of the prototype robot, a second design was developed with the slope of 30° . For this design directly printing the cantilever leg as a quadrilateral cross-section with a slope of 30° along one edge would significantly stiffen the leg, such that attaching piezoelectric ceramic strip on the surface may not produce required actuation for the motion of the bot. For this design, then, the entire leg surface plane was tilted at an angle of 30° . Figure 3(b) shows the rendered image of prototype bot with a leg surface inclination of 30° .

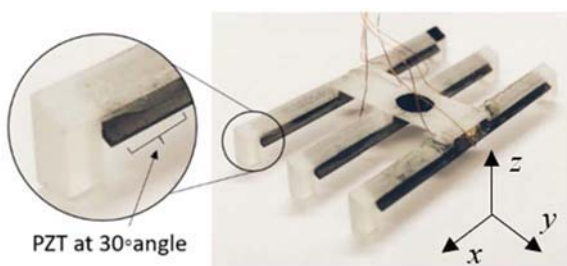


Fig. 1. Sample prototype robot with piezoelectric unimorph assembly at 30° angle. Robot is 20 mm long by 30 mm wide.

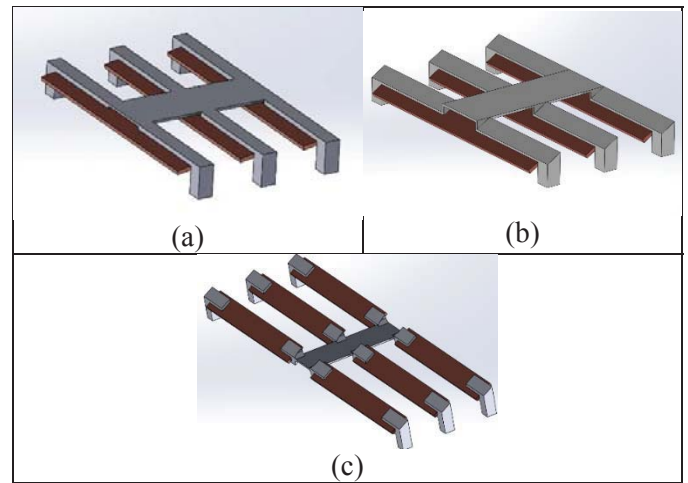


Fig. 2. Robot designs for empirical testing: (a) planar legs with 10° PZT tilt; (b) 30° leg and PZT tilt; (c) 30° , individually operated legs.

TABLE I. PARAMETERS OF FABRICATED PROTOTYPES

Features	3 PZT 10°	3 PZT 30°	6 PZT 30°
Mass [g]	1.19	1.1	2.14
Body length [mm]	20	20	20
Body width [mm]	7	7	7
Body and leg thickness [mm]	0.3	0.3	0.3
Number of legs	6	6	6
Leg length [mm]	12.5	12.5	35
Leg width [mm]	2	2	2
Piezoelectric elements	3	3	6
Foot length [mm]	3.65	3.65	3.65
Foot width [mm]	2	2	2
Foot thickness [mm]	2	2	2

In each of the above designs, actuation is performed using three piezoelectric ceramic strips, with each strip shared by a pair of two legs to keep robot size small and limit leg-to-leg variability. To study the performance of the tilted-leg robots when each leg is actuated separately, a third robot design was developed as shown in Fig 2(c). It uses six piezoelectric ceramic strips each one of the six legs. Here the main rigid body and the foot are attached only through the support of the piezoelectric ceramic strip. This iteration on the design was made to study how motion and performance is affected without any stiffness due to the leg thickness.

B. Fabrication

The reference (planar) robot design based on [1] and the robot with 10° tilted legs were printed with an inexpensive, extrusion-based 3D printer (Ultimaker 2.0). However, extrusion-based desktop 3D printer has a limitation in producing surfaces at angles without other support. Due to this constraint on fabrication the other two robot designs 2 and 3 were fabricated using a ProJet 3500 HDMax 3D printer which uses MultiJet printing technology to print parts at resolution as small as $16 \mu\text{m}$. This also makes the robot frame nearly defect free which is very hard to avoid on the parts printed through extrusion [3], though this complicates direct comparison of experimental results across designs. Figure 3 shows images of all three fabricated and assembled prototype bots. Table 1 lists

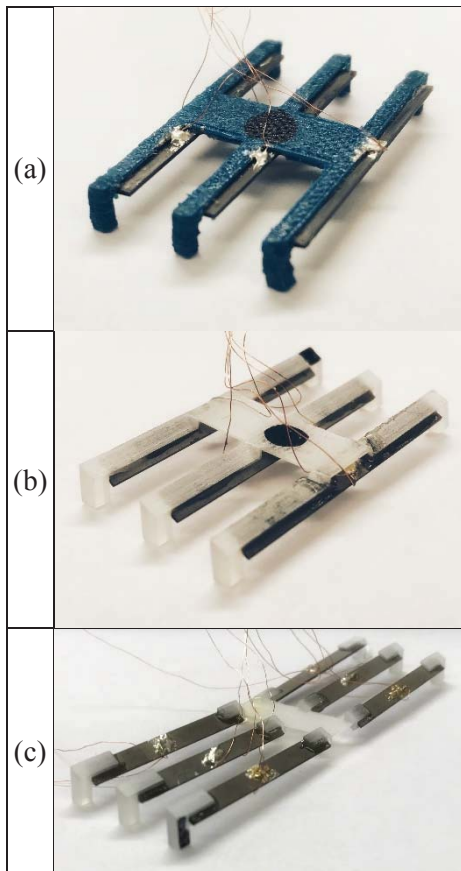


Fig. 3. Completed prototypes of tilted leg piezoelectric robots: (a) planar legs with 10° PZT tilt; (b) 30° leg and PZT tilt; (c) 30°, individually operated legs.

major feature dimensions of the assembled tilted leg robots.

III. EXPERIMENTAL SETUP

The prototype robots were tested for their performance for walking/running at various leg actuation frequencies and voltages, with emphasis on low-voltage operation. All tests were formed on a wooden surface, with robot velocity measured using a camera (60 fps with 1080 resolution). Figure 4 shows the schematic diagram of the experimentation setup. An RF signal generator was used to generate desired input signal to actuate the attached piezoelectric ceramic strips. A laser Doppler vibrometer (LDV) was used to measure leg motion. LDV measurements in this paper are taken with the robot held stationary in air by its chassis, though foot or body motion during locomotion can also be measured for brief periods as the robot passes under the laser. An oscilloscope was used to view and record the input signal supplied to the prototype bot and output signal from the LDV.

Robots were wired differently depending on their design. For robots using three piezoelectric strips across six legs, front and rear piezoelectric strips were connected to the same terminal (Fig. 5a) and the center strip/legs were connected to the other terminal of the power supply. This configuration gave better results for forward motion mode than other combinations of leg connections (i.e., all on same terminal (Fig. 5b) or front or rear

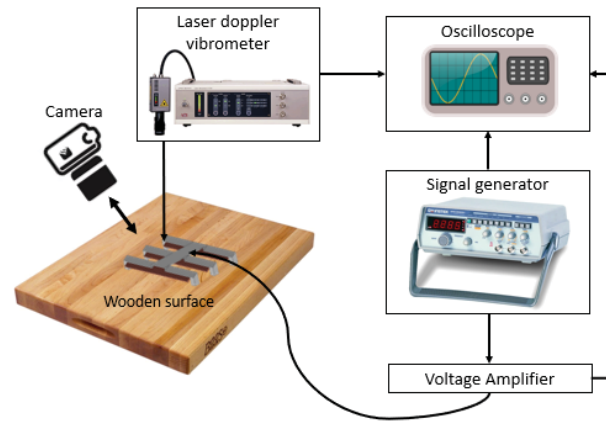


Fig. 4 Schematic diagram of experimentation setup

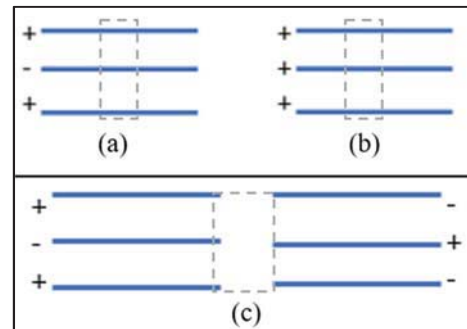


Fig. 5. Sample wiring schemes for robot testing (a) alternating 3-PZT; (b) shared 3-PZT; (c) tripod 6-PZT.

opposite to others). For the robot using six piezoelectric strips a tripod configuration was used (Fig. 5c).

Initial testing was performed to determine the frequency range at which bots could achieve successful locomotion. In this step, all testing was done with a 10 V square wave. The speed of the bots was determined when they were maximum for an optimal frequency using video recordings of the bot behavior. After determining the best-performing prototype, that robot was tested for speed performance with increased voltages. Best actuation frequency for speed was determined at each voltage supply by tuning the input square wave. The velocity of the prototype robot was determined by video capture and analysis with Tracker software, which uses predefined marker on a moving object to determine its displacement, velocity and acceleration. Running was consistently achieved up to 80 V; at higher voltages the prototype robot jumps in an aggressive manner and speed became difficult to measure. This is believed to be the point at which decent from one step coincides with initiation of the next step, leading to resonant hopping but with poor repeatability due to impact variations. It should also be noted that speed measurement accuracy is reduced as velocity increases, due to more limited numbers of frames while the robot is in the field of view.

Finally, the motion profiles of the prototype robot feet were determined at various frequencies using the LDV. The laser was directed at the surfaces of individual robot legs, and the vibration amplitude and velocity were extracted. Data was collected for motion in both vertical direction and horizontal directions in

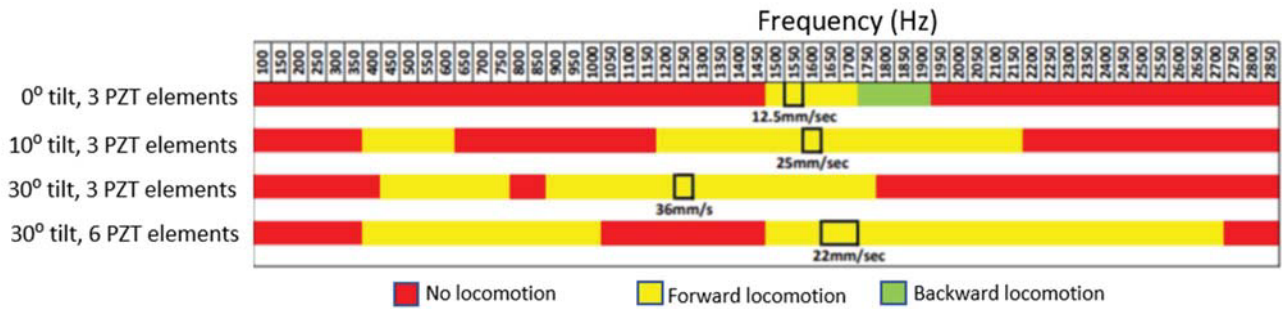


Figure 6. Overview of excitation frequencies producing measurable locomotion with 10 V input, and operating points at which maximum speeds were observed for prototype robots and a fully-planar robot baseline. Due to time constraints, absolute speeds have been recorded only at certain frequencies, but quantified trends for other prior prototypes have been reported in [1].

the time domain. This data was processed using MATLAB to convert leg displacement in both axes as a function of time and generate phase plots of motion.

IV. RESULTS

Figure 6 gives an overview of the performance of the prototype robots when legs were excited at 10 V, though speed at most frequencies has not yet been fully quantified. The red region indicates there was no motion at the corresponding frequency. The yellow region indicates there was motion in forward direction at the corresponding frequency and green indicates backward motion at the corresponding frequency. The black box indicates the best performance of robot over the range of frequencies tested. Locomotion Speed

Robots were tested from 100 Hz to 3000 Hz with the 10V square wave input to the PZT strips. As a point of reference, the first set of tests was performed with a planar robot (0° leg tilt, 3 PZT elements over 6 legs), similar to those reported in [1]. As can be seen in Fig. 6, this robot only showed forward motion over a narrow frequency range with a 10V input, from 1.5 kHz to 1.7 kHz. And at 1.5kHz the best performance speed was around 12.5mm/s. This is near the second resonant frequency of the robot legs, based on frequency response data. Despite the low speed, one benefit of the planar design is the ability to move forward or backward: from a frequency of 1.75 kHz to 1.9 kHz this robot moved backwards as change in phase of multiple modal contributions reverses the lateral direction of the robot feet at impact.

The first tilted-leg robot, with three piezoelectric strips at an angle of 10°, achieved forward locomotion over a wider range of actuation conditions than the planar bot. It first achieves forward locomotion near the first leg resonance, from 400 Hz to 600 Hz. It then also achieves forward motion from 1.2 kHz to 2.15 kHz. The best performance was found in high frequency range at 1.6 kHz with speed of around 25mm/sec.

Similar results were seen for the robot with three piezoelectric strips at an angle of 30°. The low frequency range for forward locomotion was from 450 Hz to 750 Hz and the high frequency range was from 900 Hz to 1.75kHz. Best performance was observed at 1.25kHz, at a speed of approximately 36 mm/s. Sample screenshots for this robot are shown in Fig. 7.

The robot with six piezoelectric strips at an angle of 30°, utilizing a tripod gait, had the widest low frequency range from 400 Hz till 1 kHz, indicating most effective locomotion with the

first resonant mode of the legs. It exhibited a higher frequency locomotion range from 1.55 kHz to 2.7k kHz. However, robot speed was reduced, with best speed was 22mm/sec at 1.6-1.7 kHz, possibly due to the increased mass of the robot, or reduced symmetry between the legs.

The results show that as the piezoelectric strip angle of inclination increases the speed performance of the prototype bot improves dramatically, at least for comparably sized robots. Also, there are common trends in frequency response; as angle increases the range of effective input frequencies widens and shifts towards lower frequency which may be better for the robot structure and future battery use, reducing fatigue and actuation cycles.

Figure 8 shows the results of testing the fastest low voltage robot (3 PZT strips at 30°) at increasing voltage levels. It is seen from the results that increasing voltage supply improves locomotion speed significantly, reaching speeds as high as 400 mm/s, or approximately 20 body lengths per second, before irregular robot jumping behavior arose. The voltage speed relation is not linear, likely due to reduced effectiveness of ground contact and possibly nonlinearity in the piezoelectric and/or 3D-printed materials. It was found the frequency of the input signal giving the highest speeds remained constant with increasing voltage supply.

A. Foot Motion Profiles

Various studies have been done on small organisms and robots to understand effective gaits, i.e. [19], [20]. Vibratory robots have some limitations in terms of interpretation in this way due to reliance on distributed elastic vibratory motion with light damping and limited stroke length. To perform some qualitative interpretation of leg motion profiles (i.e. amplitude, lateral vs. vertical contributions, and timing), foot motion profiles were measured from the prototype robots. While foot displacement with ground impact will be substantially different from that in air, some observed trends may be drawn from nominal foot motion at various frequencies.

Figure 9 shows the motion profiles of a sample foot from each tilted-leg robot when actuated near the frequency producing greatest locomotion speeds in their low and high frequency operating regions (near first and second resonances, respectively). With increased leg tilt increased lateral amplitudes are achieved, as would be expected for generating faster forward walking. More effective operating conditions (i.e. 30° tilts, near higher-order resonances) appear to be

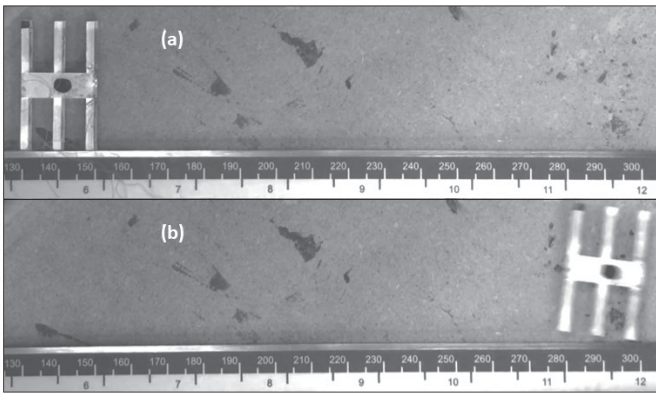


Figure 7. Screen capture at (a) 0s and (b) 1.167 s of robot with three PZT elements at 30° leg tilt, excited with 20 V square wave input at 1670 Hz.

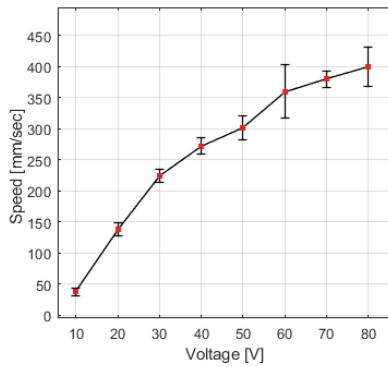


Figure 8. Robot speed versus input voltage to hexapod with 3 PZT strips at 30° angle, driven with a 1.25 kHz square wave.

associated with more elliptical foot motions, which would seem to indicate agreement with predictions from more general hexapod gait studies. Interestingly, amplitudes of foot motion near the second leg resonances show comparable amplitudes to those near first resonances. This would not be expected for an ideal cantilever beam, which suggests that more analysis of the robots' foot and body contributions to overall vibratory mode shapes is required. This is potentially the largest contribution to higher speeds near second resonances, as comparable range of motion at higher frequencies will, all else being equal, produce faster gaits. Furthermore, lower frequency profiles generally show more irregularity (i.e. Fig 9(a), 9(c)), attributed to excitation of higher-frequency modes. In past work, irregular motion has been observed to produce worse locomotion outcomes, due to inconsistent foot strike angles and/or impact timing [18].

B. Energy Requirements

With successful locomotion using just three small PZT strips at 10 V, energy and power consumption of the prototype robots can be brought close to that of millimeter-scale robots based on thin-film piezoelectric materials. The total capacitance of the PZT strips in the three element robots is less than 30 nF, compared to a typical total capacitance of approximately 10 nF in thin-film piezoelectric micro-robots [17] [21]; millimeter-

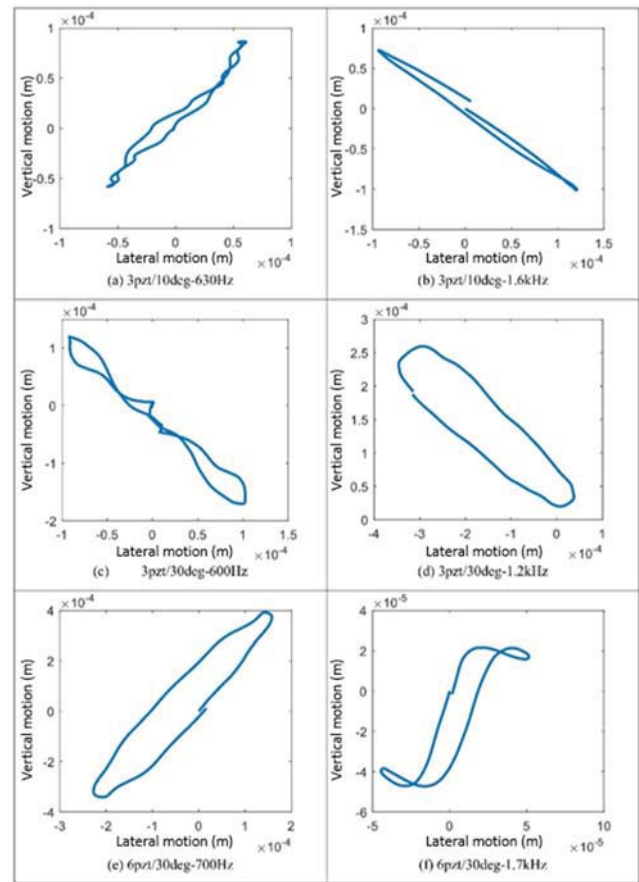


Figure 9. Robot foot motion profiles (y-z plane) in air near first (left column) and second (right column) resonances. Robots with (a) 10° leg tilt, 3 PZT elements at 630 Hz; (b) 10° tilt, 3 PZT elements at 1.6 kHz; (c) 30° tilt, 3 PZT elements at 600 Hz; (d) 30° tilt, 3 PZT elements at 1.2 kHz; (e) 30° tilt, 6 PZT elements at 700 Hz; (f) 30° tilt, 6 PZT elements at 1.7 kHz

scale robots feature much smaller PZT actuator areas, but PZT thin-film thicknesses (~1 μm) keep capacitance relatively large. Such thin-film robots also operate at relatively low voltages (10-20 V) as large electric fields can be generated over the film thickness. Projected operating frequencies for thin-film robots are also in the range of hundreds of Hz to a few kHz [22]. This makes one of the most important potential contributions of the robots tested here being to serve as testbeds for batteries, electronics, and control systems that might eventually be translated to micro-scale walking robots.

Compared to other centimeter-scale robots, power consumption remains an advantage of the proposed architectures. At 10 V operation, power consumption is approximately 1.4 mW to move at 1.8 body lengths per second. At 80 V, 92 mW are required to move at 20 body lengths per second. This exceeds prior piezoelectric robots and is similar even to the motor-driven DASH robot at 15 body lengths per second [9]. However, the robots in this work provide about an order-of-magnitude lower weight-bearing capacity compared to the DASH robot and other more power intensive designs.

C. Limitations

The above work is by no means either an exhaustive study of robot design options, nor at this time does it explore in depth the physical phenomena or dynamics that produce observed robot behavior. The primary benefit of the work above is to reduce voltage requirements while maintaining good locomotion speed compared to past piezoelectric robots of similar construction, bringing certain features more closely in line with smaller, millimeter-scale robots under development based on microelectromechanical system (MEMS) technologies. Future work will involve more thorough dynamic modeling and characterization of robot locomotion, and integration of compact power supplies based on solid-state batteries for open-loop, untethered operation.

Current results also face a variety of limitations on interpretation, given that only experimental evaluation on a finite number of robot geometries has been conducted to date. The effects of payload, and whether added payload may be more influential on one type of leg geometry than another has not been assessed. Installation of a power source and its associated mass will likely reduce advantages in power requirements of these robots compared to past, untethered systems. In addition, there is a mismatch in material sets and printing resolution between from the 0° and 10° robot designs to the 30° robot design, which may slightly exaggerate the benefits of the latter design. Finally, full details of speed versus frequency and further tilting of leg geometries to higher angles have not yet been examined.

V. CONCLUSIONS

This study was undertaken to improve the performance of simple rapid-prototyped robots based on piezoelectric actuation. It is shown that tilting robot legs can greatly increase robot performance, in terms of speed and/or voltage requirements, of this class of robots used to study vibratory robot dynamics, gait development, and power management. Speeds of up to approximately a body length per second at 10 V, or much higher speeds at higher voltages, have been achieved. While absolute speed is moderate by standards of robots at this scale, locomotion is achieved with an energy profile reasonably similar to that of smaller, millimeter-scale robots, enabling use of these designs as testbeds for power source and energy management strategies intended for even smaller robot development.

At the centimeter-scale, further gait improvement may be possible by developing the mathematical models for these designs' dynamics and determining the optimal angle of inclination for the piezoelectric strip, material selection, and foot geometry. In addition, compliance of the robot chassis may play a substantial role in the performance of the tested robots, and there may be value in exploring the behavior of the bot when the chassis is made stiffer or more compliant. Motion profile studies with ground impact remain to be done to fully understand robot performance.

REFERENCES

- [1] J. Qu, C. Teeple and K. Oldham, "Modeling legged microrobot locomotion based on contact dynamics and vibration in multiple modes and axes," *ASME Journal of Vibration and Acoustics*, vol. 139, p. 031013, 2017.
- [2] J. Qu and K. Oldham, "Multiple-mode dynamic model for piezoelectric micro-robot walking," in *ASME International Design Engineering Technical Conferences*, Cleveland, OH, 2016.
- [3] A. DeMario and J. Zhao, "A miniature, 3D-printed, walking robot with soft joints," in *ASME International Design Engineering Technical Conferences*, Cleveland, OH, 2017.
- [4] J. Rajkowski, A. Garratt, E. Schaler and S. Bergbreiter, "A multi-material milli-robot prototyping process," in *IEEE/RSJ International Conference on Robots and Systems*, St. Louis, MO, 2009.
- [5] N. Bartlett, M. Tolley, J. Overvelde, J. Weaver, B. Mosadegh, K. Bertoldi, G. Whitesides and R. Wood, "A 3D-printed, functionally graded soft robot powered by combustion," *Science*, vol. 349, no. 6244, pp. 161-165, 2015.
- [6] J. Gul, B.-S. Yang, Y. Yang, D. Chang and K. Choi, "In situ UV curable 3D printing of multi-material tri-legged soft bot with spider mimicked multi-step forward dynamic gait," *Smart Materials and Structures*, vol. 25, p. 115009, 2016.
- [7] A. Baisch, P. Sreetharan and R. Wood, "Biologically-inspired locomotion of a 2g hexapod robot," in *IEEE/RSJ International Conference on Intelligent Robots and Systems*, Taipei, Taiwan, 2010.
- [8] K. Hoffman and R. Wood, "Myriapod-like ambulation of a segmented microrobot," *Autonomous Robots*, vol. 31, pp. 103-114, 2011.
- [9] P. Birkmeyer, K. Peterson and R. Fearing, "DASH: A dynamic 16g hexapedal robot," in *IEEE International Conference on Intelligent Robots and Systems*, St. Louis, MO, 2009.
- [10] A. Dharmawan, H. Hariri, S. Foong, G. Soh and K. Wood, "Steerable miniature legged robot driven by a single bending unimorph actuator," in *IEEE Intl. Conference on Robots and Systems*, Tokyo, Japan, 2017.
- [11] S. Rios, A. Fleming and Y. Yong, "Miniature resonant ambulatory robot," *IEEE Robotics and Automation Letters*, vol. 2, pp. 337-343, 2017.
- [12] H. Hariri, L. Prasetya, S. Foong, G. Soh, K. Otto and K. Wood, "A tether-less legged piezoelectric miniature robot using bounding gait locomotion for bidirectional motion," in *IEEE International Conference on Robotics and Automation*, Stockholm, Sweden, 2016.
- [13] R. Fukui, A. Torii and A. Ueda, "Micro robot actuated by rapid deformation of piezoelectric elements," in *International Symposium on Micromechanics and Human Science*, 2001.
- [14] B. Lambrecht, A. Horchler and R. Quinn, "A small insect-inspired robot that runs and jumps," in *Proceedings of the IEEE International Conference on Robotics and Automation*, Barcelona, Spain, 2005.
- [15] J. Pulskamp, "Millimeter-scale MEMS enabled autonomous systems," in *Proceeding of the SPIE: Micro- and Nanotechnology Sensors, Systems, and Applications*, Baltimore, MD, 2012.
- [16] K. Oldham, J. Pulskamp, R. Polcawich, P. Ranade and M. Dubey, "Thin-film piezoelectric actuators for bio-inspired micro-robotic applications," *Integrated Ferroelectrics*, vol. 54, no. 1, pp. 54-65, 2007.
- [17] J. Choi, M. Shin, R. Rudy, C. Kao, J. Pulskamp, R. Polcawich and K. Oldham, "Thin-film piezoelectric and high-aspect ratio polymer leg mechanisms for millimeter-scale robotics," *International Journal of Intelligent Robotics and Applications*, vol. 1, no. 2, pp. 180-194, 2017.
- [18] J. Ryou and K. Oldham, "Dynamic characterization of contact interactions of micro-robotic leg structures," *Smart Materials and Structures*, vol. 23, p. 055014, 2014.
- [19] J. Schmitt, M. Garcia, R. Razo, P. Holmes and R. Full, "Dynamics and stability of legged locomotion in the horizontal plane: a test case using insects," *Biological Cybernetics*, vol. 86, no. 5, pp. 343-353, 2002.
- [20] J. Collins and I. Stewart, "Hexapodal gaits and coupled nonlinear oscillator models," *Biological Cybernetics*, vol. 4, no. 287-298, p. 68, 1993.
- [21] K. Teichert and K. Oldham, "Modeling cyclic capacitive loading of thin-film batteries," *Journal of the Electrochemical Society*, vol. 164, no. 2, pp. A360-A369, 2017.
- [22] J. Qu, J. Choi and K. Oldham, "Dynamic structural and contact modeling for a silicon hexapod microrobot," *ASME Journal of Mechanisms and Robotics*, vol. 9, p. 061006, 2017.